COMPDYN 2015
5th ECCOMAS Thematic Conference on
Computational Methods in Structural Dynamics and Earthquake Engineering
M. Papadrakakis, V. Papadopoulos, V. Plevris (eds.)
Crete Island, Greece, 25–27 May 2015

FINITE ELEMENT INVESTIGATION OF A NEW SEISMIC ENERGY ABSORPTION DEVICE THROUGH SIMOULTANEOUSLY YIELD AND FRICTION

Magdalini D. Titirla[1] **and Panikos K. Papadopoulos**[1]

[1] Department of Civil Engineering
Aristotle University of Thessaloniki, Greece
e-mail: {mtitirla, paniko}@civil.auth.gr

Keywords: Passive Energy Dissipation System, Finite Element Method, Absorption Seismic Energy, Friction.

Abstract. *The aim of this study is to investigate the micro-behavior of the CAR1 device. This device was presented by Papadopoulos et al [1] and has the advantages to (i) provide additional stiffness as well as (ii) absorption of seismic energy, (iii) provide control of the axial forces that are developed at the diagonal steel rods. Last but not least, it has the ability to retain the plastic displacements to a desired level. The first step was to model and analyze the group of superimposed blades in order to ascertain its behavior under monotonic loading, increased step by step until the collapse. To that purpose, Finite Element (FE) models of the system were developed and analyzed using the software ABAQUS. Parametric investigation was conducted to define the optimum combination of number and thickness as well as their elastoplastic properties. Furthermore, the group of superimposed blades was modeled and analyzed under quasi static cyclic loading, in order to ascertain its behavior to absorbed seismic energy. In addition, numerical results were compared with the same experimental so as to validate the model in the software ABAQUS.*

1 INTRODUCTION

The safety of construction (existing or new) is one of the major priorities of engineering globally, because structures often subject to large and often devastating, for their viability, loadings. So, great interest is in the study of the innovations of the design and materials of construction that minimize the probability of failure of the structure in any charging. Therefore, many efforts have been made to create devices that will absorb the majority of the seismic energy but will not belong to the supporting structure of the construction. The main advantages of these, is the easy replaced or repaired. These devices belong to the passive energy dissipation systems, do not require external power to generate system control forces and hence, are easy and cheap to implement in a structure. Passive energy dissipation devices such as visco-elastic dampers, metallic dampers and friction dampers have widely been used to reduce the dynamic response of civil engineering structures subjected to seismic loads [2, 3] Their effectiveness for seismic design of building structures is attributed to minimizing structural damages by absorbing the structural vibratory energy and by dissipating it through their inherent hysteresis behaviour [2].

In order to demonstrate the effectiveness of the devices, many passive energy dissipation systems were studied in experimental research [4, 5, 6, 7], others in numerical research [8, 9, 10] and others in both of these.

The Finite Element Method (FEM) has become the most popular method in both research and industrial numerical simulations. Several algorithms, with different computational costs, are implemented in the finite codes, such as ABAQUS [11], which is commonly used software for finite element analysis. Understanding the nature, advantages and disadvantages of this software, ABAQUS has been chosen to validate the group of the superimposed blades, which is the main element of the investigated device. Numerical analysis was conducted in order to investigate the behavior of the superimposed blades. What is more, a micro-investigation locally in regions of high importance is permissible. In this way, results come out that are harder to obtain experimentally.

In present paper, an analytical investigation of the group of the superimposed blades is presented through finite element analysis with parametric study of material, dimensions and friction coefficient between surface contacts.

2 DESCRIPTION OF THE INVESTIGATED DEVICE CAR1

The device CAR1, presented by Papadopoulos et al [1], is illustrated in Figure 1. The relevant movement between the exterior tube (Element A) and the interior shaft (Element B) is carried out by an elastoplastic bending deformation of the superimposed blades that connect crosswise elements A and B. The number and the dimensions of superimposed blades as well as their elastoplastic properties define the principle of elastoplastic behavior of the diagonal bars on an axial load.

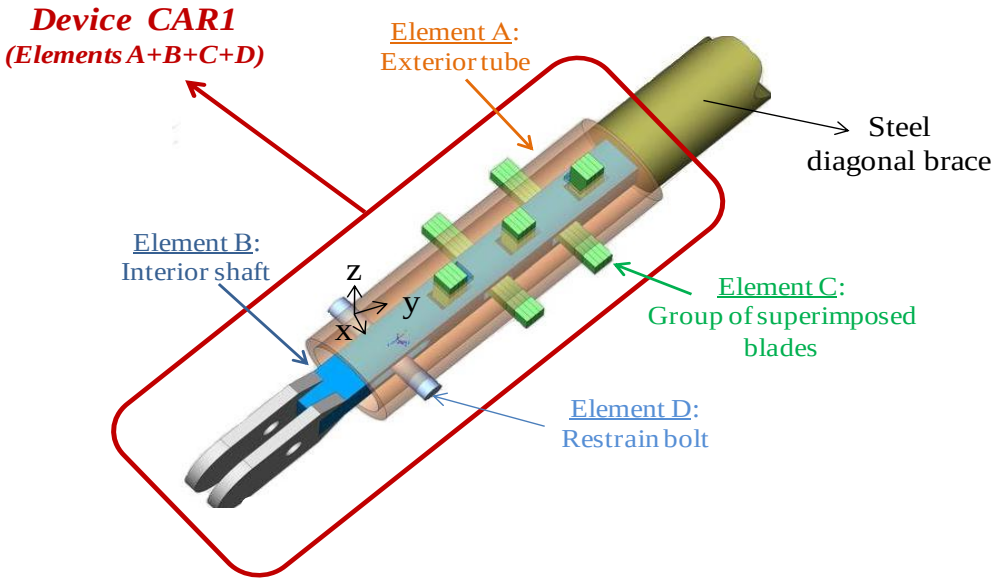

Figure 1: The investigated device CAR1.

3 FINITE ELEMENT MODELING IN ABAQUS

The finite elements analysis calibration study included modeling of a group of superimposed steel blades, with dimensions 125x20x20mm, as illustrated in Figure 2. The group consists of five steel blades with thickness of 4mm each one. Young's modulus is given as E=200GPa, Poisson's ratio is ν=0.30 and Yield strength is F=235MPa. The average coefficient of friction between steel surfaces is equal to μ=0.40 [12].

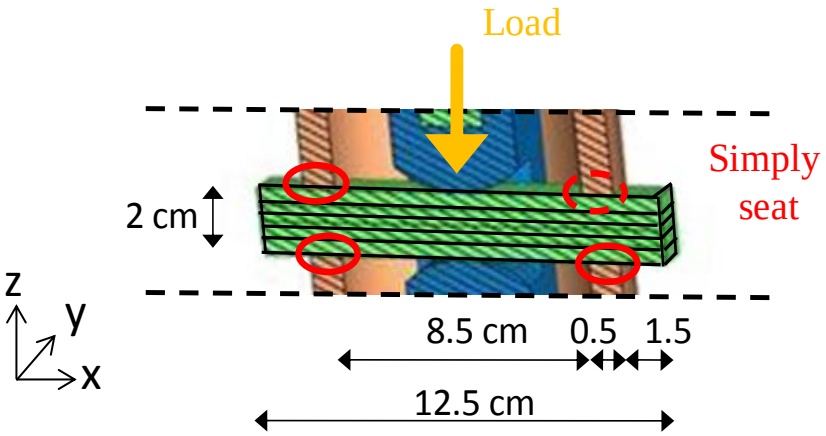

Figure 2: Description of the group of superimposed steel blades.

The superimposed blades are free to move along the axis x-x, independently of each other. The movements along the axis y-y and z-z are prohibited because of the existence of the external tube (Element A). Definition of boundary conditions for the superimposed blades is not considered necessary as simply mounted to the rigid components of the exterior tube A of the device. On the other hand, each rigid element is fixed (all degrees of freedom).

The load is transferred to the center of the top superposed blade through the interior shaft of the device (Element B). The curvature of the interior shaft leading to uniform load transfer small amplitude along the axis x-x and y-y, which be considered as a point load. During the

modeling in order to avoid high stress concentration at individual points, the load introduced as uniform in a small strip (Figure 3a). During the analysis the load imposed at a very slow pace, increased step by step until the collapse.

To simulate the behavior of the group of superimposed steel blades, it was selected to use an explicit dynamic solver because this allows the definition of very general contact conditions for complicated contact problems, without generating numerical convergence difficulties. Moreover, an explicit dynamic solver uses a consistent large-deformation theory that can model large rotations and large deformations, which is beneficial for the analysis of the group of superimposed steel blades.

For the explicit method, 3D reduced integration solid element C3D8R (eight-node bricks) are used. A view of the finite element mesh is displayed in Figure 3b.

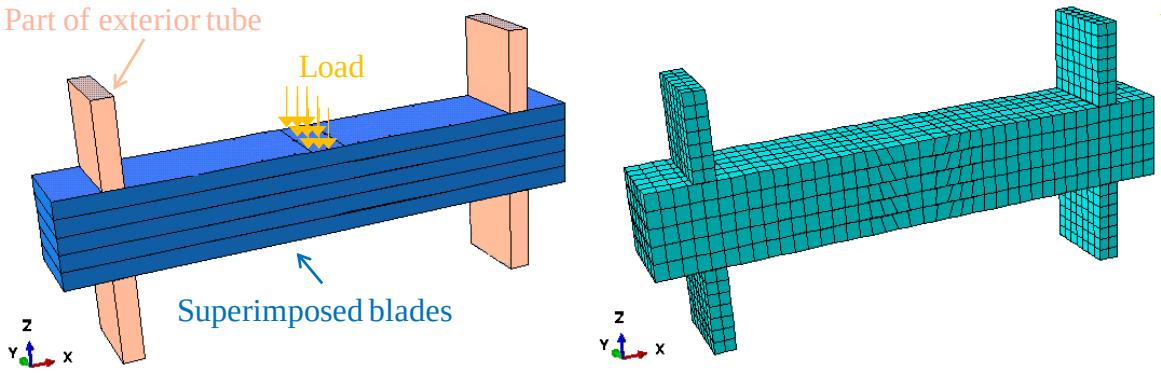

Figure 3: a) Numerical model in ABAQUS, b) Finite element mesh in ABAQUS.

Surfaces in contact are not only the interior surfaces of the superimposed steel blades, but also the part of exterior tube in which blades simply seat. Figure 4 shows all the contact surfaces with green color. To model the contact areas in ABAQUS, surface to surface contact was used with coefficient of friction equal to μ=0.40.

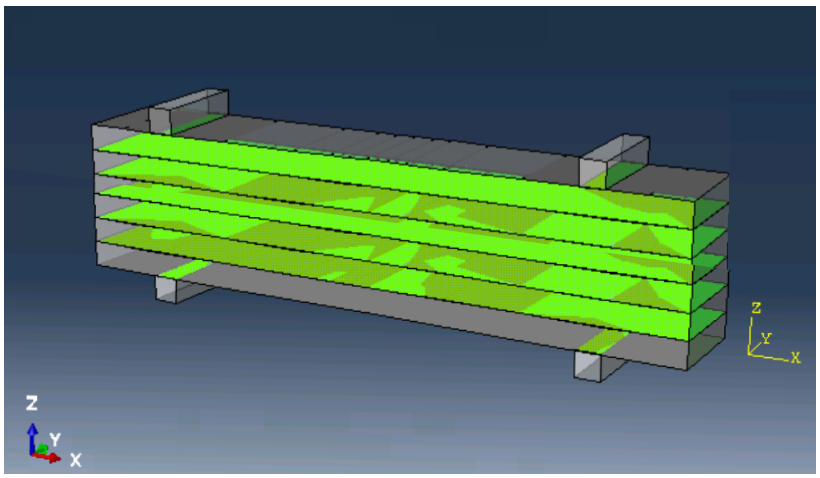

Figure 4: In contact surfaces.

Figure 5 illustrate the force-deformation relation at the central section of the bottom blade, for the group of superimposed which was presented previously, under increasing step by step load until the collapse.

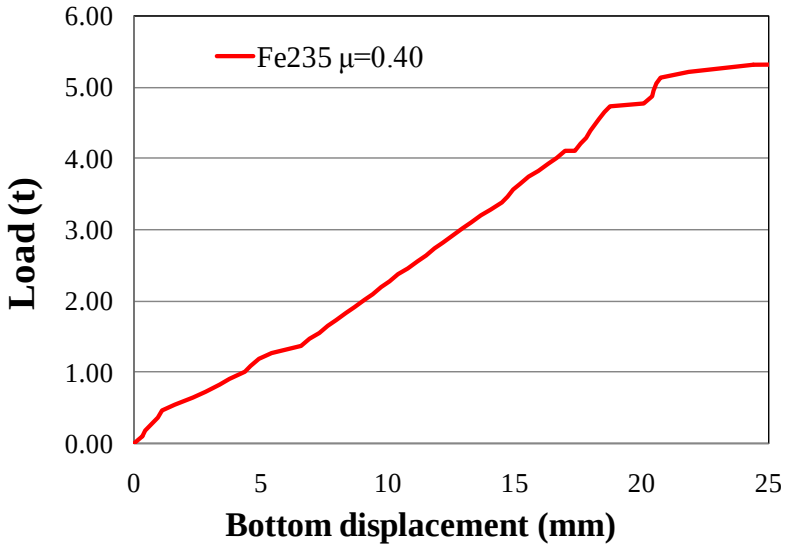

Figure 5: Numerical results with increasing step by step load until the collapse.

4 PARAMETRIC STUDY

In order to investigate the behavior of the superimposed blades 56 parametric numerical analyses have been done. The main parameters for comparison of the group of superimposed blades are: (i) the material of the blades, (ii) their thickness and (iii) the friction coefficient between contact surfaces.

4.1 Material of the blades

Three different qualities of materials were investigated, two steel and one brass. It was chosen soft qualities of steel and brass and particularly qualities that are easily founded in the commercial without order. In ABAQUS software a typical elastic-plastic material was used with properties that are presented in the following Table (Table 1) both for steel and brass.

	Young Modulus (GPa)	**Mass Density x1000 (kg/m^3)**	**Yield Stress (MPa)**	**Plastic Strain (MPa)**
Steel (Fe150)	201	7.85	150	180
Steel (Fe235)	201	7.85	235	340
Brass (Br)	100	8.45	200	370

Table 1: Elastoplastic characteristics of materials.

4.2 Thickness of the blades

The total thickness of the superimposed blades should be equal to 20mm, to satisfy the dimensions of the device CAR1. Thickness and number of the blades was classified into two categories. In the first, the material remained the same throughout the group, while in the second the material was differentiated from blade to blade. The analyzed combinations presented in Table 2. The total number of combination due to the thickness, taking account of the material, is 21.

Thickness and number of blades					Number of combination
Fe150		**Fe235**		**Br**	
20mm (1)	**or**	20mm (1)	**or**	20mm (1)	3
10mm (2)	**or**	10mm (2)	**or**	10mm (2)	3
5mm (4)	**or**	5mm (4)	**or**	5mm (4)	3
4 mm (5)	**or**	4mm (5)	**or**	4mm (5)	3
2 mm (10)	**or**	2mm (10)	**or**	2mm (10)	3
5mm (2)	**or**	5mm(2)	**and**	5mm(2)	2
4mm (3)	**or**	4mm(3)	**and**	4mm(2)	2
5 mm (3)	**or**	5mm(3)	**and**	2.5mm (2)	2

Table 2: Number and thickness of groups of superimposed blades.

4.3 Coefficient of friction

When surfaces in contact move relative to each other, the friction between the two surfaces converts kinetic energy into thermal energy. Friction is not itself a fundamental force but arises from interatomic and intermolecular forces between the two contacting surfaces. The coefficient of friction (COF), often symbolized by the Greek letter μ, is a dimensionless scalar value which describes the ratio of the force of friction between two bodies and the force pressing them together. The coefficient of friction depends on the materials used as Table 3 illustrates.

Surfaces in contact	Coefficient of friction μ
Steel to Steel	0.00 (theoretical smooth)
Steel to Steel	0.40 (standard)
Steel to Steel	0.70 (knurled)
Brass to Brass	0.00 (theoretical smooth)
Brass to Brass	0.40 (standard)
Steel to Brass	0.35 (standard)

Table 3: Coefficient of friction between contact surfaces.

5 DISCUSSION OF PARAMETRIC STUDY

Figure 6 illustrates the observed dependence of load on displacement (at the middle point of the bottom blade) for group of superimposed steel blades for all coefficient friction. The groups, which presented in this Figure, are one blade with thickness 20mm and two blades with thickness equal to 10mm each one. It can be deduced that the blades of both groups entered in the plastic area in small displacements. The behavior of these groups is not compatible with the rationale of the device CAR1, although the large load that can be received.

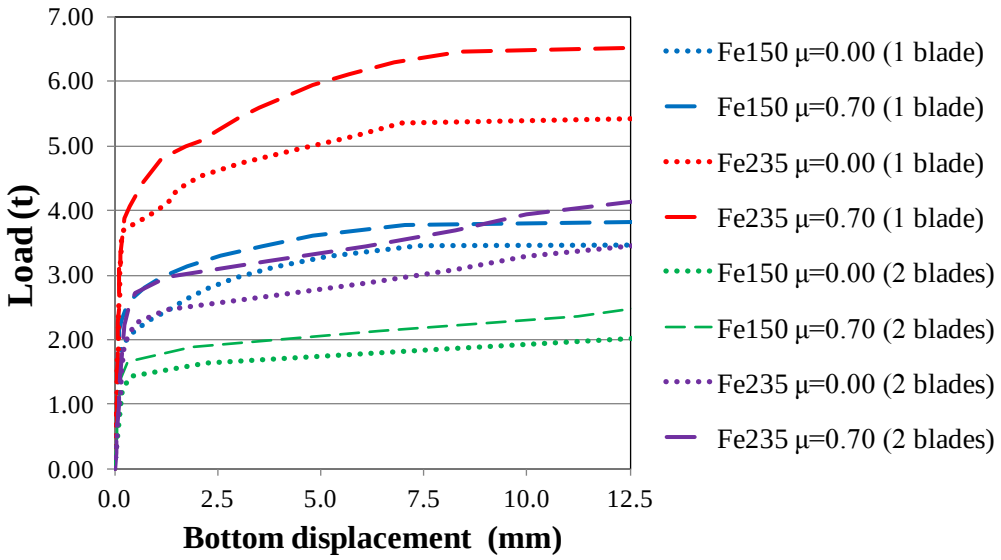

Figure 6: Load versus displacement for group with blade's thickness 20mm and 10mm.

The observed dependence of load on displacement (at the middle point of the bottom blade) for group of superimposed steel blades with thickness 4mm for all coefficient friction is presented in Figure 7. Also for the desirable displacement of 13mm, we can notice the variation of the received load. The choice of movement was indicative in order to observe the influence of the coefficient of friction. Thus creating knurled in blades, such as increasing the friction coefficient to 0.70, the received force for this movement can easily increased around 20%.

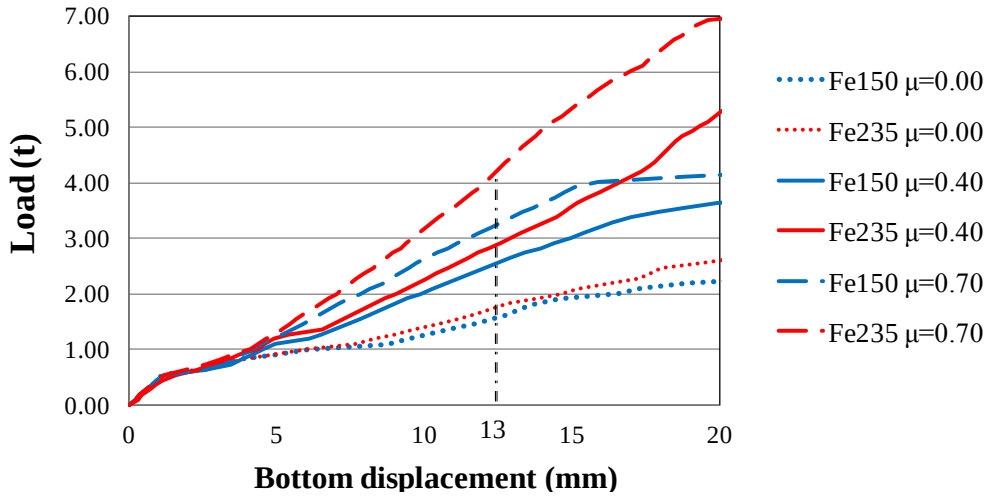

Figure 7: Load versus displacement for group with blade's thickness 4mm.

Figure 8 shows the comparison of maximum load for the desirable displacement equal to 13mm. Three different thicknesses of blades, such as 5mm, 4mm and 2mm, were selected in Figure 8a. The materials of the groups are steel and brass. It is necessary to notice that material and thickness remain the same into the group. The optimum combinations are the groups with blade's thickness 5mm or 4mm and material Fe235. The received load for the brass blades is small due to the Young Modulus. In addition, the material was differentiated from blade to blade in Figure 8b. The received load is smaller than the corresponding with the same material into the group, but it reduces the probability to behavior like one part over time.

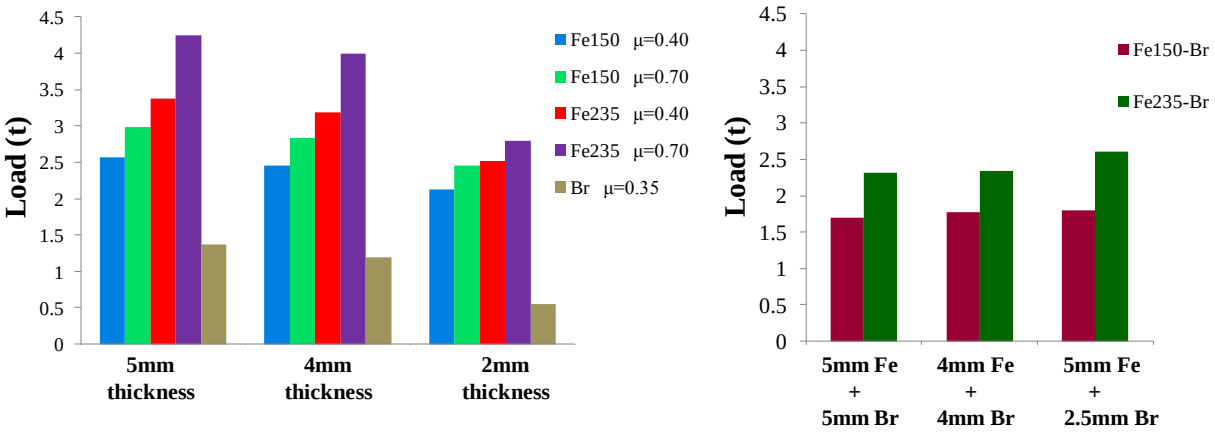

Figure 8: Maximum load for the desirable blades' displacement of 13mm.

One of the optimum combinations was chosen to illustrate the variation of the mises stress according to friction coefficient at a load magnitude corresponding to yield of frictionless group (Figure 9). The thickness of the blades is equal to 5mm and the material is Fe235.

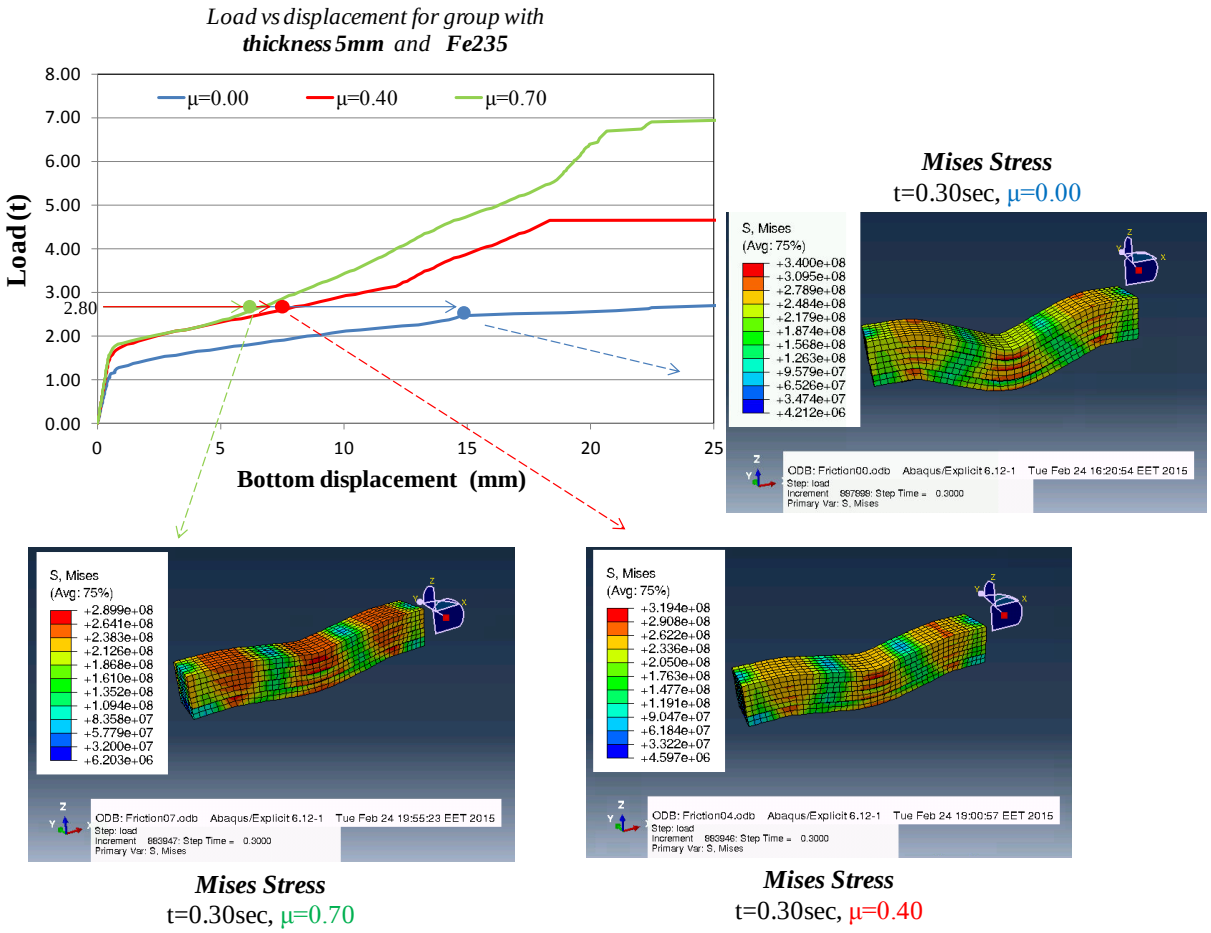

Figure 9: Load versus displacement for superimposed blades with thickness equal to 5mm and Fe235 and mises stress of blades at a load magnitude corresponding to yield of frictionless group.

6 CYCLIC LOADING

Quasi-static cyclic tests were carried out for a group of superimposed steel blades in order to ascertain its behavior to absorbed seismic energy. Multiple dynamic tests were run on each group of superimposed blades under varying load amplitudes and time. In Figure 10 the cycling load versus time, for the group of 4 blades with thickness equal to 5mm, is presented. Blue line illustrate one cycle loading with stable maximum force equal to 2.25t, while red line shows three cycles loading with increasing force cycle by cycle from 1.50t to 2.25t.

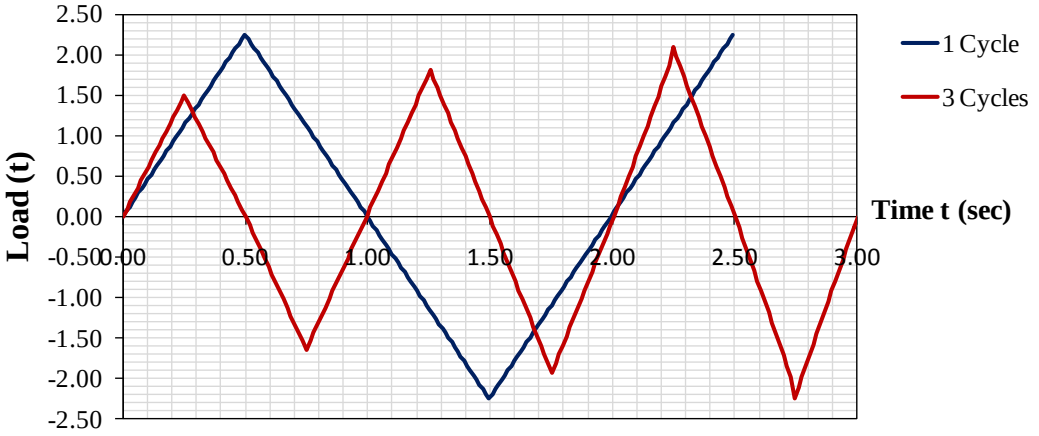

Figure 10: Quasi static cycling load versus time.

Figure 11 illustrates the hysteretic loops of the displacement for the previous cycles loading. As hysteretic loops of the displacement represent the amount of the absorbed energy, we can notice the ability of the device CAR1 to absorb seismic energy. From the shape and consistency of the hysteresis loops, it can be determined that the CAR1 device is effective in dissipating energy. The area within a hysteresis loop is equivalent to the amount of energy that the device is dissipating.

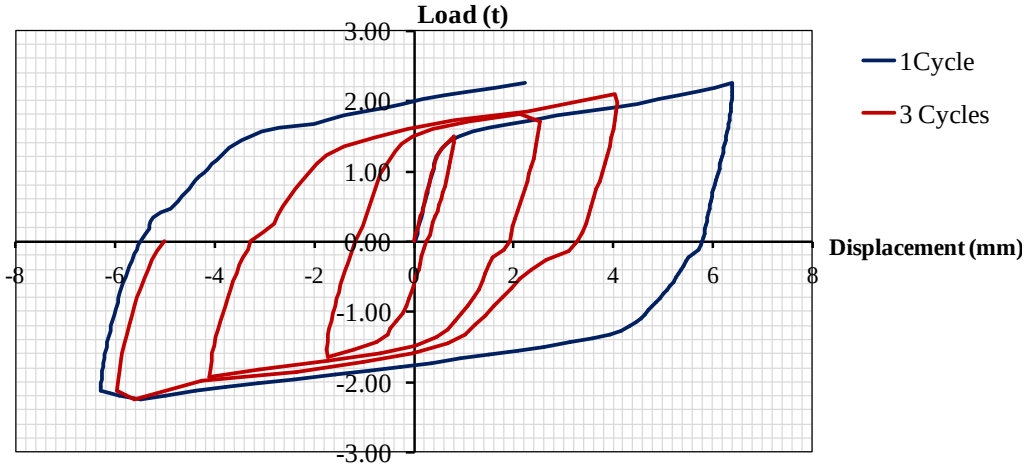

Figure 11: Hysteretic loops.

In addition, tests were run for ten cycles in order to ascertain any degradation in behavior over repeated cycles. To produce these hysteresis loops, load of amplitudes varying from 2.50t-3.00t were applied on group for 10 cycles as shown in Figure 12.

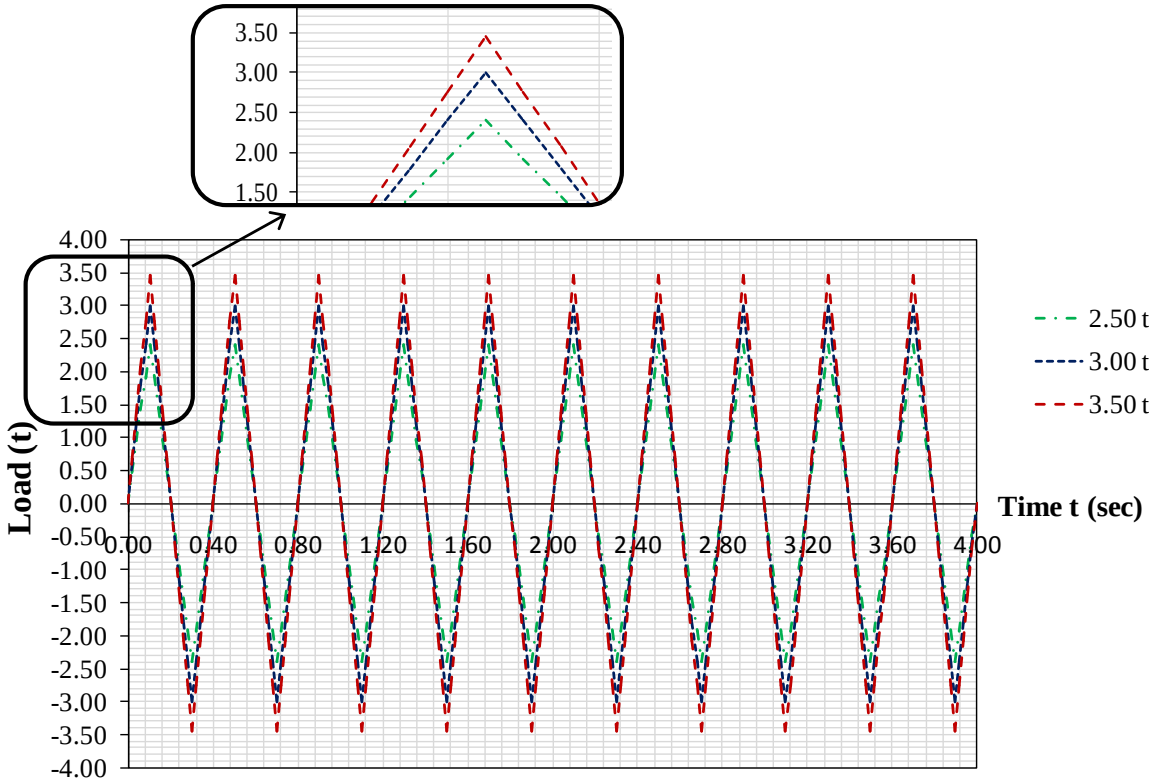

Figure 12: Cycling load versus time for ten cycles.

From the shape and consistency of the hysteresis loops, as illustrated in Figure 13, it can be determined that the CAR1 device is effective in dissipating energy and it will not break down during the course of cyclic loading. Furthermore, it can be seen that CAR1 device has very good energy dissipation potential.

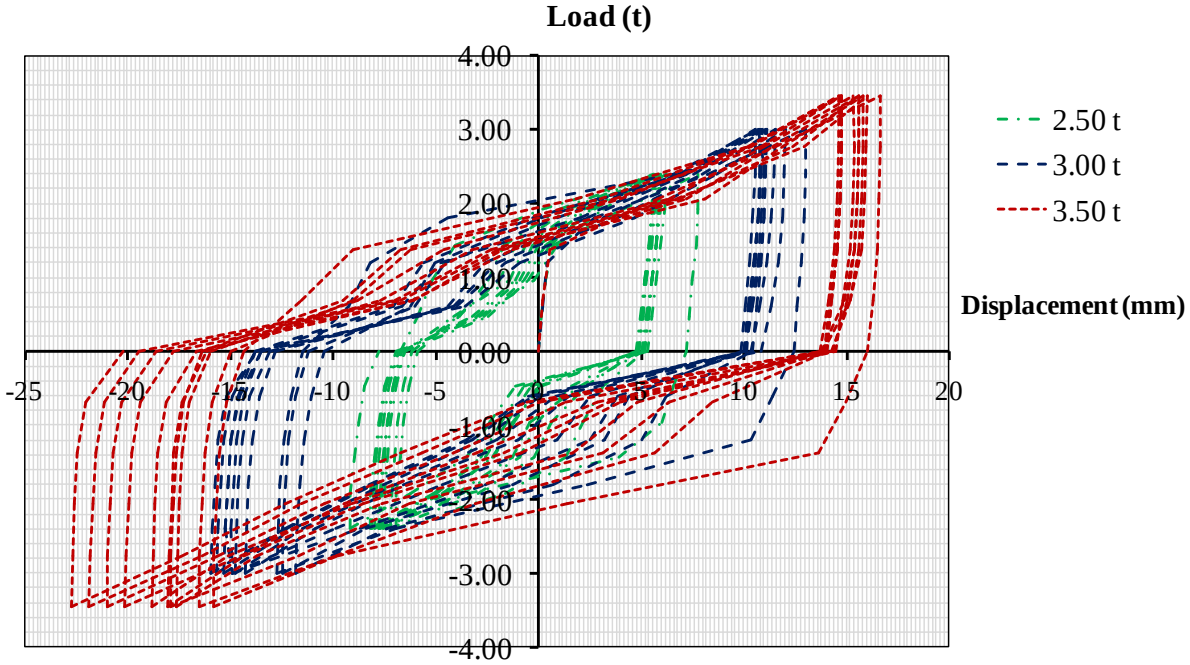

Figure 13: Hysteretic loops.

Figures 14 shows the distribution of plastic equivalent strain and the deformed shape of the 5 superimposed steel blades with thickness 4mm at the end of 10 cycles. It is observed that the nodes with more stress, is the center of the blades and the support points of the blades into the exterior tube.

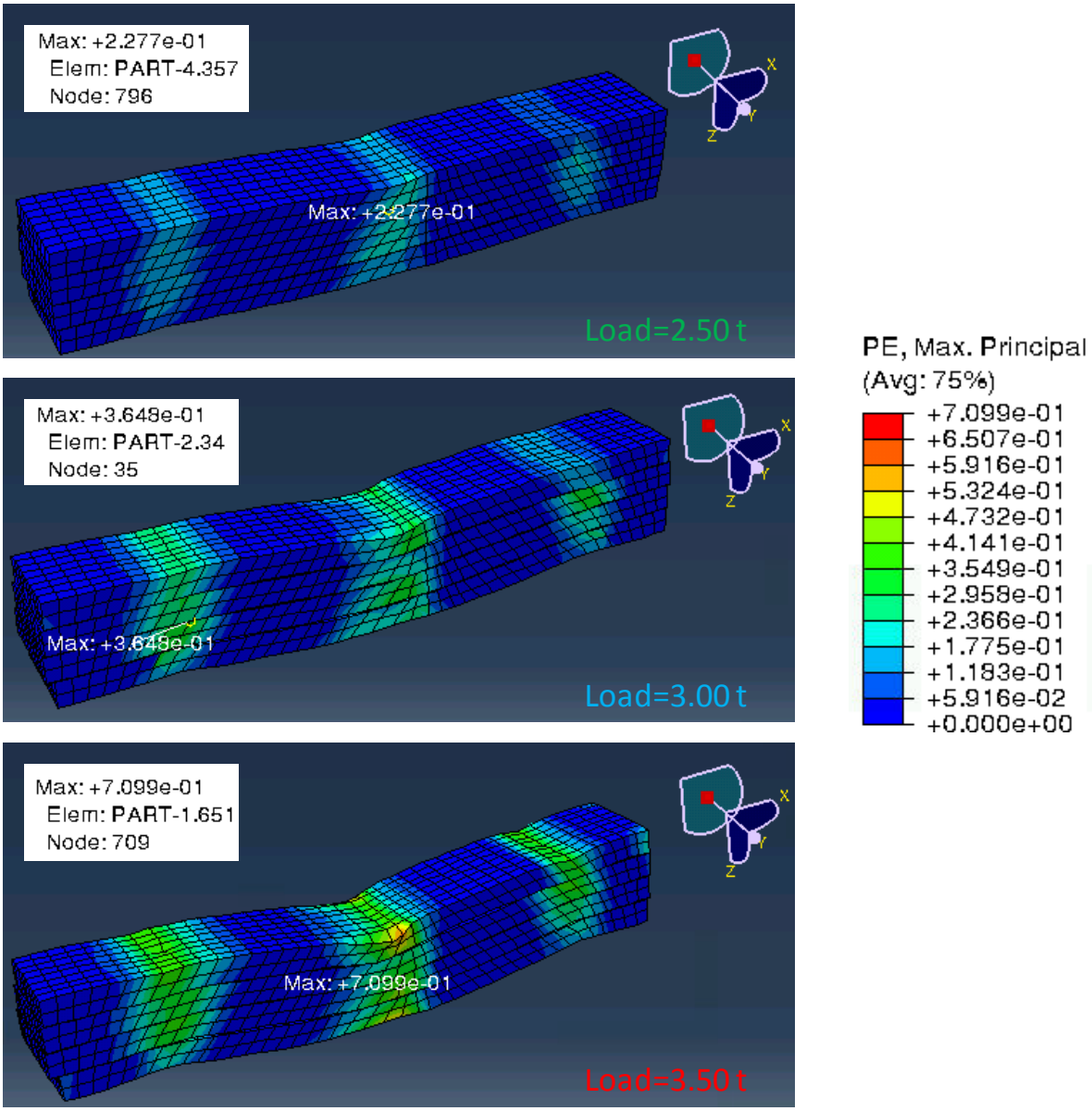

Figure 14: Deformed geometry from a group of 5 superimposed blades at the end of 10 cycles.

7 VALIDATION OF NUMERICAL AND EXPERIMENTAL TEST RESULTS

The finite elements analysis calibration study included: (i) modeling of a group of superimposed steel blades and (ii) comparison of the numerical results with the same experimental. The group consists of five steel blades, 4mm thick each. Young's modulus is given as E=200GPa, Poisson's ratio is ν=0.30 and Yield strength is F=235MPa. The average coefficient of friction between steel surfaces is equal to μ=0.40. During the analysis the load imposed at a very slow pace, increased step by step until the load of 3.60t and then reduced step

by step. As it is shown, in Figure 15, the finite element results are in accordance with the experimental results.

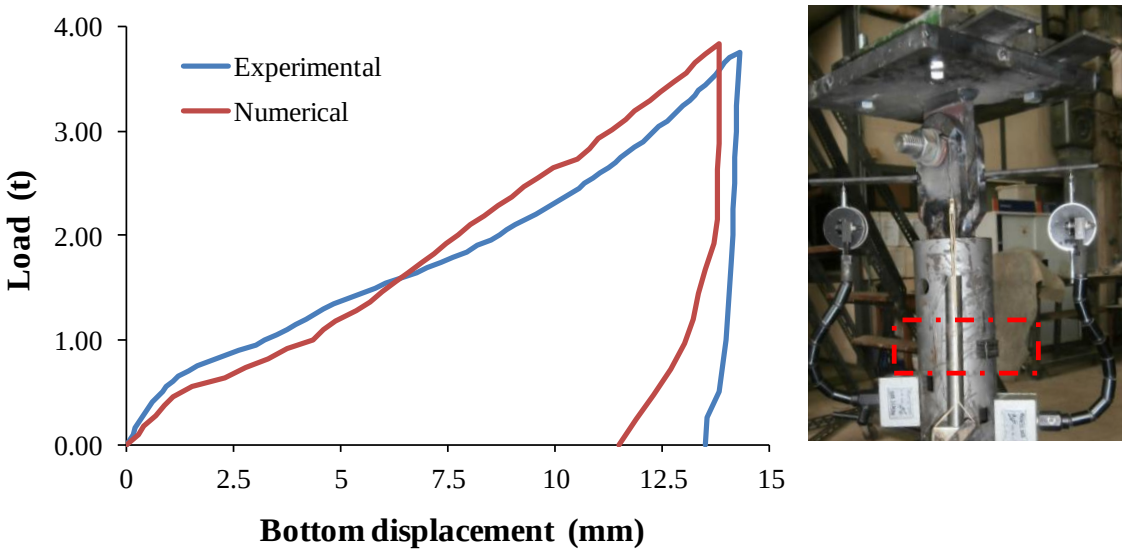

Figure 15: Experimental and numerical test results.

8 CONCLUSION

In this paper, an analytical investigation of the group of the superimposed blades, which is the main element of the device CAR1, was presented. The group analyzed through finite element analysis with parametric study of material, dimensions and friction coefficient between surface contacts. Furthermore, the numerical results reveal some conclusions of the behavior of the superimposed blades, namely that:

- ✓ Group of blades with thickness 20mm and 10mm entered in the plastic area in small displacements. The behavior of these groups is not compatible with the rationale of the device CAR1, although the large load that can be received. While blades with thickness equal to 4mm and 5mm are the optimum combinations.

- ✓ In addition, in group blades where the material was differentiated from blade to blade the received load is smaller than the corresponding with the same material into the group, but it reduces the probability to behavior like one part over time.

- ✓ The hysteresis loops of the displacement for the 10 cycles loading confirm the ability of the device CAR1 to absorb seismic energy. The area within a hysteresis loop is equivalent to the amount of energy that the device is dissipating. From the hysteresis loops, it can be seen that the device CAR1 not only is effective in dissipating energy, but also it will not break down during the course of cyclic loading.

ACKNOWLEDGMENTS

The authors would like to thank Alkis Papadopoulos, PhD Candidate at Aristotle University of Thessaloniki, for his valuable support provided during the experiments. Although the experiments results are thesis of other research, these were helpful to validate the numerical results.

REFERENCES

[1] P.K. Papadopoulos, M.D. Titirla, A.P. Papadopoulos, A new seismic energy absorption device through simultaneously yield and friction used for the protection of structures. *2nd European Conference on Earthquake Engineering and Seismology*, Istanbul, Turkey, August 25-29, 2014.

[2] T.T. Soong, B.F.S Jr, Supplemental energy dissipation: state-of-the-art and state-of-the-practice. *Engineering Structures*, **24**, 243-259, 2002.

[3] I.D. Aiken, D.K. Nims, J.M. Kelly, Comparative study of four passive energy dissipation systems. *Bull. N. Z. Natl. Soc. Earthquake Engineering*, **25**, 175–192, 1992.

[4] I.D. Aiken, D.K. Nims, A.S. Whittaker, J.M. Kelly, Testing of passive energy dissipation systems. *Earthquake spectra*, **9**, 335-370, 1993.

[5] G. Anagnostides, A.C. Hargreaves, Shake table testing on an energy absorption device for steel braced frames. *Soil Dynamics and Earthquake Engineering*, **9**, 120-140, 1990.

[6] P.K. Papadopoulos, T.N. Salonikios, S.A. Dimitrakis, A.P. Papadopoulos, Experimental investigation of a new steel friction device with link element for seismic strengthening of structures. *Structural Engineering & Mechanics*, **46**, 487-504, 2013

[7] A.S. Whittaker, V.V. Bertero, J.L. Alonso, C.L. Thompson, Earthquake Simulator Testing of Steel Plate Added Damping and Stiffness Elements. *Report No. UCB/EERC 89/02*, University of California, Berkley, 1989.

[8] A.S. Pall, Friction devices for aseismic design of buildings, *4th Canadian Conference on Earthquake Engineering*, Vancouver, Canada, 1983.

[9] P. Papadopoulos, New nonlinear anti-seismic steel device for the increasing the seismic capacity of multi-storey reinforced concrete frames. *The structural design of tall and special buildings*, **21**, 750-763, 2012.

[10] J.D.M. Ramirez, L. Tirca, Numerical Simulation and Design of Friction- Damped Steel Frame Structures damped. *15th World Conference in Earthquake Engineering*, Lisbon, Portugal, September 24-28, 2012.

[11] ABAQUS: *Theory and analysis user's manual version 6.12*, Providence, RI, USA: Dassault Systèmes SIMULIA Corp. 2012.

[12] F. Cobb, Structural Engineers' Pocket Book. *2nd Edition, British Standards Edition*, 2008.